

A Novel Frequency-Domain Small-Signal Analysis of Resonant Power Converters

Gideon J. J. van Zyl

Abstract—A frequency-domain small-signal analysis of resonant power converters is presented. In this analysis, the load presented to the ac side of the rectifier is modeled as a time varying resistor. Using conversion matrix techniques and an iterative procedure to find the magnitude and phase of the time-varying resistor, the transfer functions of the converter can be obtained fast and accurately. An advantage of this approach is that the analysis can be carried out with the load represented in the frequency domain. This is a significant advantage when dealing with complex (e.g., plasma) loads where only measured small-signal impedance data may be available. An example demonstrating the accuracy of the method is presented.

Index Terms—Conversion matrix, frequency domain, resonant power converter, small-signal analysis, transfer function.

I. INTRODUCTION

VARIOUS methods exist for obtaining the linearized small-signal transfer functions of resonant power converters [1]–[4]. These methods all require a representation of the load by equivalent lumped components or assume a simple topology for the load.

Here, a method of determining the linearized small-signal transfer functions of resonant converters delivering power to arbitrary loads is presented. Both the converter and load are described in the frequency domain leading to a greatly simplified analysis for complex load and converter topologies. In the analysis presented here it is assumed that the converter operation is described with a reasonable degree of accuracy if only the fundamental harmonic of the switching frequency is considered.

The analysis applied to a practical series-parallel resonant converter operating above resonance is presented in Section III.

II. ANALYSIS

Consider a resonant converter delivering power to a reactive load where the converter is modulated. (Amplitude and frequency modulation are treated within the same framework.) Modulation of the converter results in a modulated load voltage. Since the load is reactive, the variation in load current is not necessarily in phase with the variation in the load voltage. When viewed from the ac side of the rectifier, the ratio of current to voltage varies at the modulation frequency. The load presented to the ac side of the rectifier, thus takes the form of a time-varying resistor. This is illustrated in Fig. 1.

Manuscript received May 9 2001; revised October 26, 2003. This paper was recommended by Associate Editor D. Czarkowski.

The author is with Advanced Energy Industries, Inc., Fort Collins, CO 80525 USA (e-mail: dvzyl@ieee.org).

Digital Object Identifier 10.1109/TCSI.2004.830690

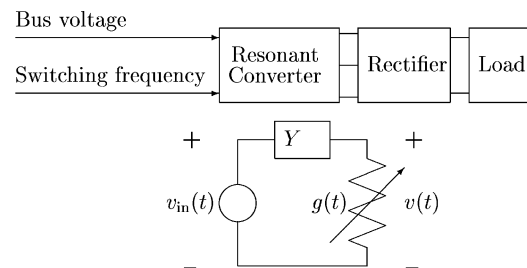


Fig. 1. Resonant converter and the representation to determine the small-signal linearized transfer function.

The analysis of the converter comprises two steps. The first step involves an accurate determination of the load presented to the converter at the nominal switching frequency and subsequently the nominal load voltage. This step is dependent on the specific configuration of the converter and the load and is outside the scope of the present discussion. (See [5] for an example of how this step might be performed in a particular case. Figs. 2 and 3 show a particular topology and the equivalent circuit for this topology.)

Assume that the first step of the analysis determined that the equivalent load presented to the converter at the nominal switching frequency consists of a resistor R_l in parallel with a capacitor C_l . (In general, the equivalent load takes the form of a resistor in parallel with either a capacitor C_l or an inductor L_l .) The converter including C_l (or L_l) is converted to a Thévenin equivalent source Y . Various convenient scaling schemes can be applied. In this case, assume that without any modulation, $v_{in}(t) = V_u \cos(\omega_0 t)$, where ω_0 is the nominal switching frequency and V_u is scaled such that the peak amplitude of the voltage v is equal to the average value of the load voltage. (e.g., in the case of a lightly loaded three phase converter the value of V_u would typically be $(4/2\pi) \times \sqrt{3} \times 0.955$ times the bus voltage.)

Let the converter be modulated at a frequency of ω_δ rad/s. Since we are interested in a small-signal analysis, we may assume that the load conductance can be expressed as $g(t) = g_{dc} + g_{ac} \cos(\omega_\delta t + \phi)$, that g_{ac} is small and that $g_{dc} = 1/R_l$.

Let y be the impulse response associated with the Thévenin equivalent source admittance Y and let $*$ denote convolution. Then, the circuit satisfies

$$v(t)g(t) = [(v_{in} - v) * y](t).$$

Using the definition

$$X(\omega) = \int_{-\infty}^{\infty} x(t)e^{-j\omega t} dt$$

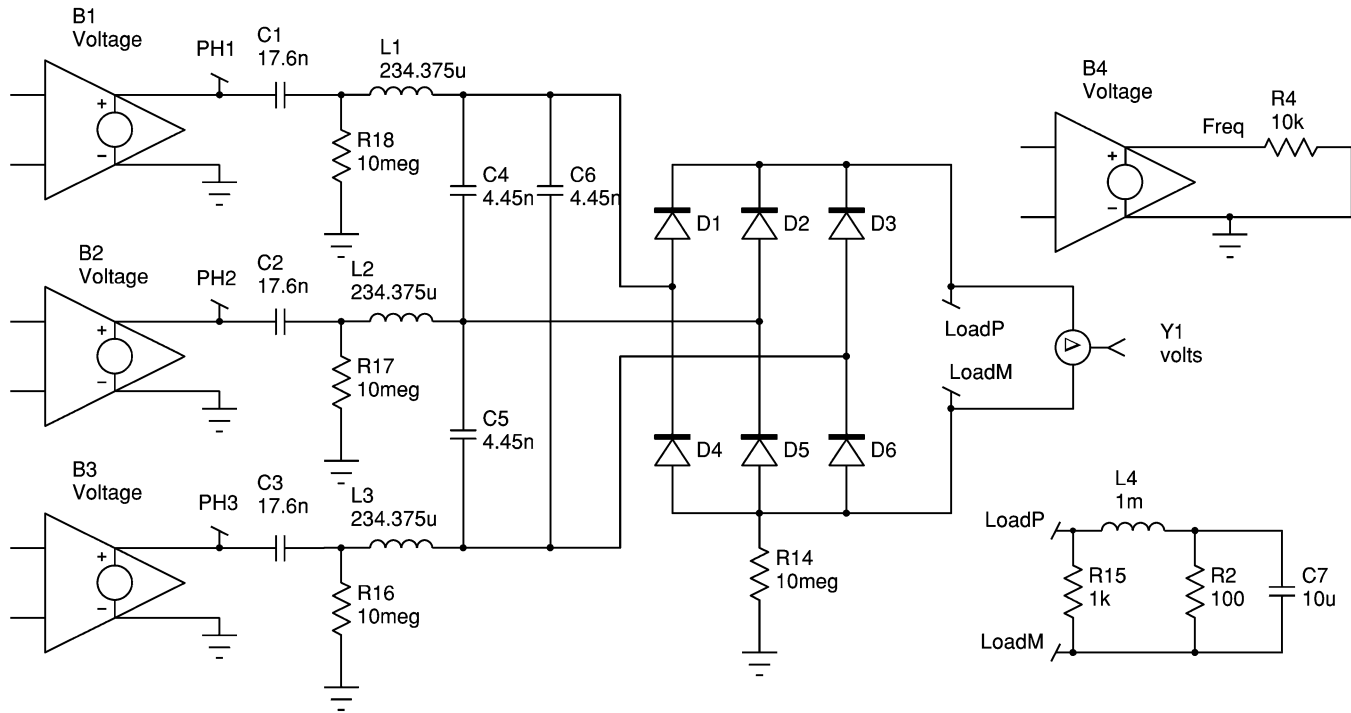


Fig. 2. Circuit used to illustrate the accuracy of the method. The independent sources B1–B3 generate modulated square waves. The source B4 generates a voltage equal to the instantaneous frequency or bus amplitude for frequency and amplitude modulation respectively. More details are given in the appendix.

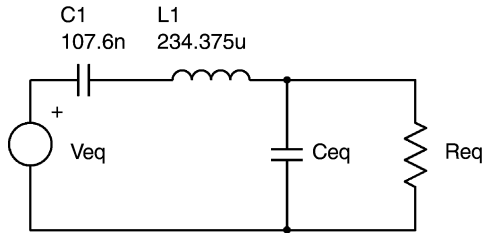


Fig. 3. Equivalent circuit for the converter of Fig. 2.

for the Fourier transform and extending the definition to distributions in the usual way, the circuit satisfies the following equation in the Fourier frequency domain

$$\frac{1}{2\pi}[V * G](\omega) = (V_{in}(\omega) - V(\omega))Y(\omega). \quad (1)$$

With the given definition of the Fourier transform, $\stackrel{\mathcal{F}}{\rightleftharpoons}$ denoting a Fourier transform pair and δ the Dirac delta or impulse distribution, $\cos(\omega_0 t) \stackrel{\mathcal{F}}{\rightleftharpoons} \pi[\delta(\omega + \omega_0) + \delta(\omega - \omega_0)]$ while $1 \stackrel{\mathcal{F}}{\rightleftharpoons} 2\pi\delta(\omega)$.

Thus

$$g(t) \stackrel{\mathcal{F}}{\rightleftharpoons} 2\pi g_{dc}\delta(\omega) + \pi g_{ac} [e^{-j\phi}\delta(\omega + \omega_\delta) + e^{j\phi}\delta(\omega - \omega_\delta)].$$

As a result of the convolution with g , V has to take the general form¹ (with the factor π introduced for convenience)

$$V(\omega) = \pi \sum_{k=-\infty}^{\infty} V_k^* \delta(\omega + \omega_0 + k\omega_\delta) + V_k \delta(\omega - \omega_0 - k\omega_\delta).$$

¹For a discussion in the context of mixer theory, see, e.g., [6].

By truncating the series, one obtains

$$V(\omega) \approx \pi \sum_{k=-N}^N V_k^* \delta(\omega + \omega_0 + k\omega_\delta) + V_k \delta(\omega - \omega_0 - k\omega_\delta).$$

This leads to²

$$\begin{aligned} & \frac{1}{2\pi}(V * G)(\omega) \\ &= \frac{1}{2\pi} \int_{-\infty}^{\infty} V(x)G(\omega - x) dx \\ &= \int_{-\infty}^{\infty} \pi \sum_{k=-N}^N (V_k^* \delta(x + \omega_0 + k\omega_\delta) \\ & \quad + V_k \delta(x - \omega_0 - k\omega_\delta)) \\ & \quad \times \left(g_{dc}\delta(\omega - x) + \frac{g_{ac}}{2} [e^{-j\phi}\delta(\omega - x + \omega_\delta) \right. \\ & \quad \left. + e^{j\phi}\delta(\omega - x - \omega_\delta)] \right) dx \\ &= \pi \sum_{k=-N}^N \int_{-\infty}^{\infty} (V_k^* \delta(x + \omega_0 + k\omega_\delta) \\ & \quad + V_k \delta(x - \omega_0 - k\omega_\delta)) \\ & \quad \times \left(g_{dc}\delta(\omega - x) + \frac{g_{ac}}{2} [e^{-j\phi}\delta(\omega - x + \omega_\delta) \right. \\ & \quad \left. + e^{j\phi}\delta(\omega - x - \omega_\delta)] \right) dx \end{aligned}$$

²In this paper, the Dirac distribution is handled nonrigorously. A rigorous treatment, e.g., treating δ as a functional on the set of compactly supported C^∞ functions and using an appropriate definition for convolution on this space, is outside the scope of the present discussion.

$$\begin{aligned}
&= \pi \sum_{k=-N}^N \left[V_k^* g_{\text{dc}} \delta(\omega + \omega_0 + k\omega_\delta) \right. \\
&\quad + V_k^* \frac{g_{\text{ac}}}{2} e^{-j\phi} \delta(\omega + \omega_0 + k\omega_\delta + \omega_\delta) \\
&\quad + V_k^* \frac{g_{\text{ac}}}{2} e^{j\phi} \delta(\omega + \omega_0 + k\omega_\delta - \omega_\delta) \\
&\quad + V_k g_{\text{dc}} \delta(\omega - \omega_0 - k\omega_\delta) \\
&\quad + V_k \frac{g_{\text{ac}}}{2} e^{-j\phi} \delta(\omega - \omega_0 - k\omega_\delta + \omega_\delta) \\
&\quad \left. + V_k \frac{g_{\text{ac}}}{2} e^{j\phi} \delta(\omega - \omega_0 - k\omega_\delta - \omega_\delta) \right].
\end{aligned}$$

We are interested in the case where v_{in} is the Thévenin equivalent source of either an amplitude or frequency modulated sinusoidal source at a modulation frequency of ω_δ . Let $T(\omega)e^{j\psi(\omega)}$ be the transfer function that converts the actual source to the Thévenin equivalent source with both T and ψ real valued. For frequency modulation at a small modulation index K_f , the actual source is represented in the time domain as

$$A \cos(\omega_0 t) + \frac{AK_f}{2\omega_\delta} \cos(\omega_0 + \omega_\delta)t - \frac{AK_f}{2\omega_\delta} \cos(\omega_0 - \omega_\delta)t$$

so that, for frequency modulation, we have

$$\begin{aligned}
V_{\text{in}}(\omega) &= \pi A \left[T(\omega_0) \left[e^{-j\psi(\omega_0)} \delta(\omega + \omega_0) \right. \right. \\
&\quad \left. \left. + e^{j\psi(\omega_0)} \delta(\omega - \omega_0) \right] \right. \\
&\quad + \frac{T(\omega_0 + \omega_\delta)K_f}{2\omega_\delta} \left[e^{-j\psi(\omega_0 + \omega_\delta)} \delta(\omega + \omega_0 + \omega_\delta) \right. \\
&\quad \left. + e^{j\psi(\omega_0 + \omega_\delta)} \delta(\omega - \omega_0 - \omega_\delta) \right] \\
&\quad \left. - \frac{T(\omega_0 - \omega_\delta)K_f}{2\omega_\delta} \left[e^{-j\psi(\omega_0 - \omega_\delta)} \delta(\omega + \omega_0 - \omega_\delta) \right. \right. \\
&\quad \left. \left. + e^{j\psi(\omega_0 - \omega_\delta)} \delta(\omega - \omega_0 + \omega_\delta) \right] \right].
\end{aligned}$$

Similarly, for amplitude modulation with modulation index K_a , we find

$$\begin{aligned}
V_{\text{in}}(\omega) &= \pi A \left[T(\omega_0) \left[e^{-j\psi(\omega_0)} \delta(\omega + \omega_0) \right. \right. \\
&\quad \left. \left. + e^{j\psi(\omega_0)} \delta(\omega - \omega_0) \right] \right. \\
&\quad + \frac{T(\omega_0 + \omega_\delta)K_a}{2} \left[e^{-j\psi(\omega_0 + \omega_\delta)} \delta(\omega + \omega_0 + \omega_\delta) \right. \\
&\quad \left. + e^{j\psi(\omega_0 + \omega_\delta)} \delta(\omega - \omega_0 - \omega_\delta) \right] \\
&\quad + \frac{T(\omega_0 - \omega_\delta)K_a}{2} \left[e^{-j\psi(\omega_0 - \omega_\delta)} \delta(\omega + \omega_0 - \omega_\delta) \right. \\
&\quad \left. + e^{j\psi(\omega_0 - \omega_\delta)} \delta(\omega - \omega_0 + \omega_\delta) \right] \left. \right].
\end{aligned}$$

In general

$$\begin{aligned}
V_{\text{in}}(\omega) &= \pi [V_{\text{in}1}^* \delta(\omega + \omega_0 + \omega_\delta) \\
&\quad + V_{\text{in}0}^* \delta(\omega + \omega_0) + V_{\text{in}-1}^* \delta(\omega + \omega_0 - \omega_\delta) \\
&\quad + V_{\text{in}-1} \delta(\omega - \omega_0 + \omega_\delta) + V_{\text{in}0} \delta(\omega - \omega_0) \\
&\quad + V_{\text{in}1} \delta(\omega - \omega_0 - \omega_\delta)]
\end{aligned}$$

where

$$[V_{\text{in}-1} \ V_{\text{in}0} \ V_{\text{in}1}] = A \left[-\frac{T(\omega_0 - \omega_\delta)K_f}{2\omega_\delta} e^{j\psi(\omega_0 - \omega_\delta)} \right. \\
\left. T(\omega_0) e^{j\psi(\omega_0)} \frac{T(\omega_0 + \omega_\delta)K_f}{2\omega_\delta} e^{j\psi(\omega_0 + \omega_\delta)} \right]$$

for frequency modulation and

$$[V_{\text{in}-1} \ V_{\text{in}0} \ V_{\text{in}1}] = A \left[\frac{T(\omega_0 - \omega_\delta)K_a}{2} e^{j\psi(\omega_0 - \omega_\delta)} \right. \\
\left. T(\omega_0) e^{j\psi(\omega_0)} \frac{T(\omega_0 + \omega_\delta)K_a}{2} e^{j\psi(\omega_0 + \omega_\delta)} \right]$$

for amplitude modulation.

We can now compare multipliers of $\delta(\omega - \omega_0 - l\omega_\delta)$ on the left and right side of (1). On the left-hand side, we have

$$\pi V_l g_{\text{dc}} + \pi V_{l+1} \frac{g_{\text{ac}}}{2} e^{-j\phi} + \pi V_{l-1} \frac{g_{\text{ac}}}{2} e^{j\phi}$$

while on the right-hand side, we have

$$\begin{cases} -\pi V_l Y(\omega_0 + l\omega_\delta), & l \notin \{-1, 0, 1\} \\ (-\pi V_l + \pi V_{\text{in}-1}) Y(\omega_0 - \omega_\delta), & l = -1 \\ (-\pi V_l + \pi V_{\text{in}0}) Y(\omega_0), & l = 0 \\ (-\pi V_l + \pi V_{\text{in}1}) Y(\omega_0 + \omega_\delta), & l = 1. \end{cases}$$

This leads to the conversion matrix equation

$$G \begin{bmatrix} V_{-N} \\ \vdots \\ V_N \end{bmatrix} = \begin{bmatrix} Y(\omega_0 - N\omega_\delta)(-V_{-N}) \\ \vdots \\ Y(\omega_0 - 2\omega_\delta)(-V_{-2}) \\ Y(\omega_0 - \omega_\delta)(-V_{-1} + V_{\text{in}-1}) \\ Y(\omega_0)(-V_0 + V_{\text{in}0}) \\ Y(\omega_0 + \omega_\delta)(-V_1 + V_{\text{in}1}) \\ Y(\omega_0 + 2\omega_\delta)(-V_2) \\ \vdots \\ Y(\omega_0 + N\omega_\delta)(-V_N) \end{bmatrix}$$

where the equation at the bottom of the page, holds, or

$$\begin{bmatrix} V_{-N} \\ \vdots \\ V_N \end{bmatrix} = M^{-1} \begin{bmatrix} 0 \\ \vdots \\ 0 \\ Y(\omega_0 - \omega_\delta)V_{\text{in}-1} \\ Y(\omega_0)V_{\text{in}0} \\ Y(\omega_0 + \omega_\delta)V_{\text{in}1} \\ 0 \\ \vdots \\ 0 \end{bmatrix}$$

where the first equation at the bottom of the next page, holds.

$$G = \begin{bmatrix} g_{\text{dc}} & 0.5g_{\text{ac}}e^{-j\phi} & 0 & \dots & 0 \\ 0.5g_{\text{ac}}e^{j\phi} & g_{\text{dc}} & 0.5g_{\text{ac}}e^{-j\phi} & 0 & \dots & 0 \\ 0 & 0.5g_{\text{ac}}e^{j\phi} & g_{\text{dc}} & 0.5g_{\text{ac}}e^{-j\phi} & 0 & \dots & 0 \\ \vdots & \vdots & \vdots & \vdots & \vdots & \vdots & \vdots \\ 0 & \dots & \dots & 0 & 0.5g_{\text{ac}}e^{j\phi} & g_{\text{dc}} \end{bmatrix}$$

Thus, if we guess what g_{ac} and ϕ are, we can calculate the spectrum of v . Since we are dealing with small perturbations, the only significant terms in the spectrum are V_{-1} , V_0 , and V_1 . Next, we calculate the change in the envelope of v . (This is a standard calculation [7].) Due to the scaling that we chose, this is the variation in the load voltage. Let the load voltage be $v_{dc} + v_{ac} \cos(\omega_\delta t + \sigma)$. Then, the load current is given by

$$v_{dc} Y_{load}(0) + |Y_{load}(\omega_\delta)| v_{ac} \cos(\omega_\delta t + \sigma + \arg(Y_{load}(\omega_\delta)))$$

where $Y_{load}(\omega)$ is the load admittance at frequency ω . This allows us to calculate a new estimate of $g(t)$, say $\hat{g}(t)$ as shown in the second equation at the bottom of the page. This expression has the general form

$$\frac{a + b \cos(t + \theta)}{c + d \cos(t + \varphi)}$$

Since d is assumed to be small in relation to c , we can expand this as a Taylor series to get

$$\begin{aligned} \frac{a + b \cos(t + \theta)}{c + d \cos(t + \varphi)} &= \frac{a + b \cos(t + \theta)}{c \left[1 + \frac{d}{c} \cos(t + \varphi) \right]} \\ &\approx \frac{1}{c} [a + b \cos(t + \theta)] \left[1 - \frac{d}{c} \cos(t + \varphi) \right] \\ &\approx \frac{a}{c} - \frac{ad}{c^2} \cos(t + \varphi) + \frac{b}{c} \cos(t + \theta) \\ &= \frac{a}{c} + |X + jY| \cos(t + \arg(X + jY)) \end{aligned}$$

where

$$\begin{aligned} X &= \frac{b}{c} \cos(\theta) - \frac{ad}{c^2} \cos(\varphi) \\ Y &= \frac{b}{c} \sin(\theta) - \frac{ad}{c^2} \sin(\varphi). \end{aligned}$$

Thus, we get the estimates $\hat{g}_{ac} = |X + jY|$ and $\hat{\phi} = \arg(X + jY)$. The argument appears circular, and indeed it is, but it can be solved numerically by defining $e(g_{ac}, \phi) = (\hat{g}_{ac} - g_{ac}, \hat{\phi} - \phi)$ and then using Newton's method with a numerically calculated Jacobian to adjust g_{ac} and ϕ until $e(g_{ac}, \phi) = (0, 0)$. Once we have a solution we also have the spectrum of v and that allows us to compute all the desired transfer functions.

III. EXAMPLE

Consider the three-phase series-parallel resonant converter shown in Fig. 2. In this circuit, PH1, PH2, and PH3 are square waves with a nominal switching frequency of 117.5 kHz. This particular switching frequency results in a large resonance

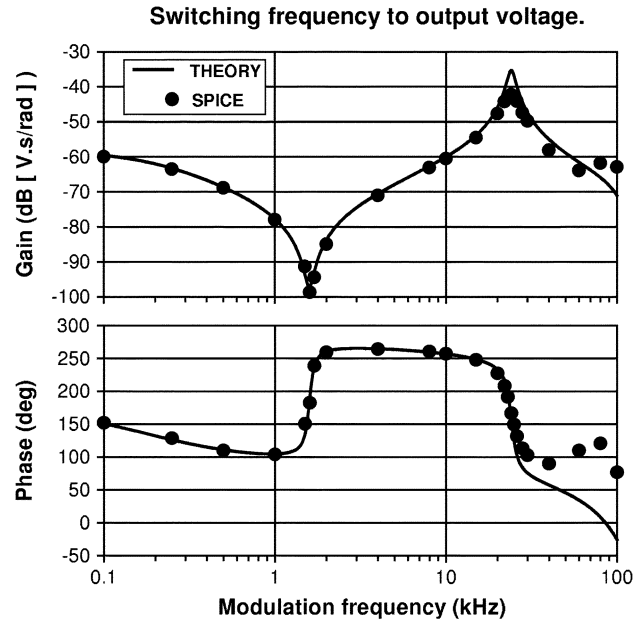


Fig. 4. Magnitude and phase of the transfer function (Output voltage/Switching frequency) V/(rad/s) for the converter of Fig. 2. The solid line is the transfer function calculated as described. The circles are the result of a Fourier analysis of a SPICE simulation as described in the appendix.

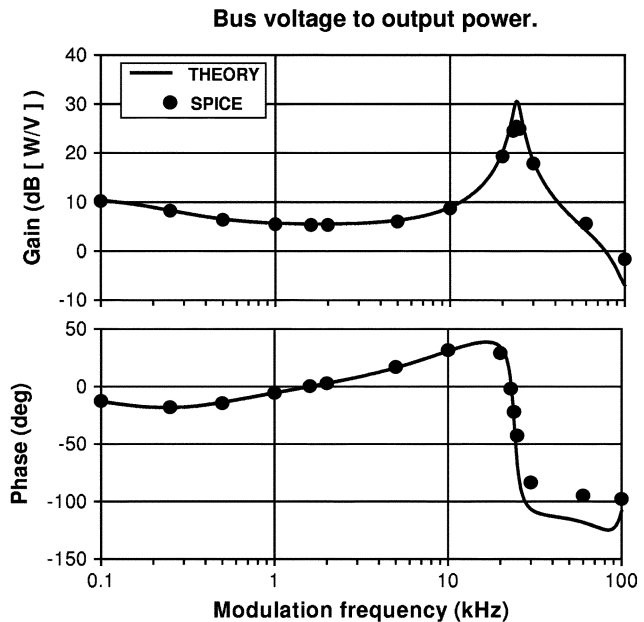


Fig. 5. Magnitude and phase of the transfer function (Output power/Bus voltage) (W/V) for the converter of Fig. 2. The solid line is the transfer function calculated as described. The circles are the result of a Fourier analysis of a SPICE simulation as described in the appendix.

$$M = G + \begin{bmatrix} Y(\omega_0 - N\omega_\delta) & 0 & \cdots & 0 \\ 0 & Y(\omega_0 - (N-1)\omega_\delta) & 0 & \cdots & 0 \\ \vdots & \vdots & \vdots & \vdots & \vdots \\ 0 & \cdots & 0 & Y(\omega_0 + N\omega_\delta) \end{bmatrix}$$

$$\hat{g}(t) = \frac{g_{dc}}{Y_{load}(0)} \frac{v_{dc} Y_{load}(0) + |Y_{load}(\omega_\delta)| v_{ac} \cos(\omega_\delta t + \sigma + \arg(Y_{load}(\omega_\delta)))}{v_{dc} + v_{ac} \cos(\omega_\delta t + \sigma)}$$

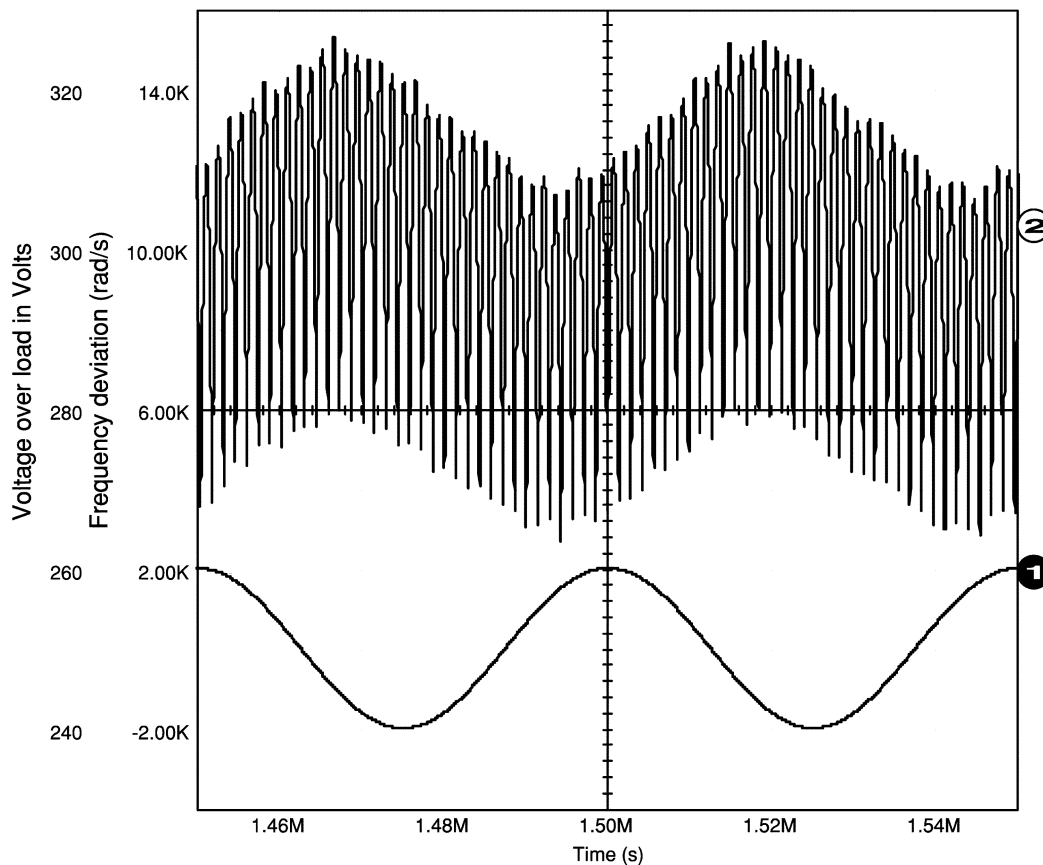


Fig. 6. The result of running the simulation with a modulation frequency of 20 kHz. The instantaneous frequency shown (labeled 1) varying between -2000 and 2000 rad/s as well as the voltage over the load are shown. Only a portion of the simulation time of 1 ms is shown.

in the frequency response, thereby making the analysis more interesting.

The equivalent circuit of the converter is shown in Fig. 3.

For this particular circuit, the scaling that needs to be applied to create a sinusoidal source such that the amplitude of the output is equal to the average load voltage is 1.053 times the bus voltage. This is the product of the factors $2/\pi$ to obtain the amplitude of the fundamental component of a square wave, the factor $\sqrt{3}$ for the three phases and the factor 0.955 to get from the peak to the average value of the output voltage. The load presented to the equivalent circuit of the converter is found to be $R_{eq} = 51.83 \Omega$ in parallel with a capacitor $C_{eq} = 18.51$ nF. (These values can be obtained using a procedure similar to that described in [5]. The values used here were found using a different method [8].)

The results of the analysis as described above compared with SPICE simulations are shown in Figs. 4 and 5. Fig. 4 shows the transfer function from a change in switching frequency to a change in load voltage while Fig. 5 shows the transfer function from a change in bus voltage to a change in power delivered to the load.

IV. CONCLUSION AND OBSERVATIONS

A new frequency-domain method for obtaining the small-signal transfer functions of resonant power converters has been presented. A significant advantage of this method is the fact that the load is represented in the frequency domain. This makes possible the use of measured load impedance data for complex loads.

It should be noted that the magnitude of the calculated transfer function is significantly higher at the resonant peaks than predicted by SPICE simulation (see, e.g., Fig. 4 at around 24 kHz.) The reason for this inaccuracy is not understood, but it is interesting to note that the same type of inaccuracy is noted in [1, Fig. 16(d)], in which a completely different approach to the problem is taken. It would be interesting to determine the reason for this inaccuracy.

A. Details of the SPICE Simulation

Time-domain simulations of the circuit shown in Fig. 2 were carried out with a maximum time step of 10 ns. Data were saved every 100 ns from 1 ms to 2 ms (up to 11 ms for low frequency modulation). To speed up the simulation, initial conditions corresponding to the nominal output voltage and current were used for C7 and L4.

For frequency modulation, the following SPICE code was used for the independent voltage sources where df is the modulation frequency in hertz (changes between simulations), fsw is the nominal switching frequency in hertz, and kf is the amplitude of the frequency deviation in radians per second.

```
.param fsw = 117.5 k
.param df = 20 k;
.param wsw = {fsw*6.283 185 31}
.param dw = {df*6.283 185 31}
.param kf = 2000;
```

```

B4 Freq 0 V = {kf} * cos({dw} * time)
B1 PH1 0 V = cos({wsw} * time + {kf/dw} * sin({dw} *
time)) > 0 ? 274.3 : -274.3
B2 PH2 0 V = cos({wsw} * (time - 2.0943951/({wsw} +
{kf} * cos({dw} * time)))+
{kf/dw} * sin({dw} * (time - 2.0943951/({wsw} +
{kf} * cos({dw} * time)))) > 0 ? 274.3 : -274.3
B3 PH3 0 V = cos({wsw} * (time - 4.1887902/({wsw} +
{kf} * cos({dw} * time)))+
{kf/dw} * sin({dw} * (time - 4.1887902/({wsw} + {kf} *
cos({dw} * time)))) > 0 ? 274.3 : -274.3

```

Fig. 6 shows the result of running the simulation with a modulation frequency of 20 kHz.

Following the SPICE simulation, the script

```

alias Vdc (v(loadp) - v(loadm))
alias Ipri (mag(@L1[i]))
alias Iload (@L4[i] + @R15[i])
alias Pwr ((@L4[i] + @R15[i]) * (V(LoadP) - V(LoadM)))
set fourgridsize = 8192
set nfreqs = 64
fourier lk v(freq) Vdc Iload Ipri Pwr

```

is run to determine the various transfer functions of interest. (The fundamental frequency of the Fourier analysis is changed so that the modulation frequency is an exact multiple of the fundamental.)

For determining the effect of a variation of the bus voltage, the SPICE code for the independent voltage sources are changed to the following. (ka is the modulation index.)

```

.param vrail = 548.6
.param fsw = 117.5k
.param df = 20k;
.param wsw = {fsw*6.28318531}
.param dw = {df*6.28318531}
.param ka = 0.04;
B4 Freq 0 V = {ka} * {vrail} * cos({dw} * time)

```

```

B1 PH1 0 V = cos({wsw} * time) > 0 ? {vrail}/2 * (1 +
{ka} * cos({dw} * time)) :
- {vrail}/2 * (1 + {ka} * cos({dw} * time))
B2 PH2 0 V = cos({wsw} * (time - 2.0943951/({wsw})) >
0 ?
{vrail}/2 * (1 + {ka} * cos({dw} * time)) : - {vrail}/2 *
(1 + {ka} * cos({dw} * time))
B3 PH3 0 V = cos({wsw} * (time - 4.1887902/({wsw})) >
0 ?
{vrail}/2 * (1 + {ka} * cos({dw} * time)) : - {vrail}/2 *
(1 + ka * cos({dw} * time)).

```

REFERENCES

- [1] V. Vorpérian and S. Cuk, "Small-signal analysis of resonant converters," in *Proc. IEEE Power Electronics Specialist Conf.*, 1983, pp. 269–282.
- [2] V. Vorpérian, "Approximate small-signal analysis of the series and the parallel resonant converters," *IEEE Trans. Power Electron.*, vol. 4, pp. 15–24, Jan. 1989.
- [3] D. Edry and S. Ben-Yaakov, "Dynamics of the capacitive-loaded push-pull parallel-resonant converter: Investigation by a spice compatible average model," in *Proc. IEEE Applied Power Electronics Conf.*, vol. 2, 1994, pp. 1035–1041.
- [4] S. Ben-Yaakov and D. Adar, Edry, "Average models as tools for studying the dynamics of switch mode dc-dc converters," in *IEEE Power Electronics Specialist Conf. Rec.*, vol. 2, 1994, pp. 1369–1376.
- [5] A. K. G. Ivensky and S. Ben-Yaakov, "A novel rc model of capacitive-loaded parallel and series-parallel resonant dc-dc converters," in *Proc. IEEE Power Electronics Specialist Conf.*, 1997, pp. 958–964.
- [6] A. A. M. Saleh, *Theory of Resistive Mixers*. Cambridge, MA: MIT Press, 1971.
- [7] P. R. Rabinovci, S. Ben-Yaakov, and S. Gluzman, "Envelope simulation by spice-compatible models of electric circuits driven by modulated signals," *IEEE Trans. Ind. Electron.*, vol. 47, pp. 222–225, Feb. 2000.
- [8] B. Hesterman, "Three-phase series resonant Wye-Wye 400 V 3 kW," Advanced Energy Ind., Fort Collins, CO, Tech. Rep., Jan. 2001.



Gideon J. J. van Zyl received the B.Eng. and M.Eng. degrees in electronic engineering and the Hon.-B.Sc. degree in mathematics from the University of Stellenbosch, Stellenbosch, South Africa, and the Ph.D. degree in electrical engineering from the University of Texas, Austin, in 1985, 1991, 1996, and 2003, respectively.

He worked for Reutech Radar Systems, Stellenbosch, South Africa from 1987 to 2001. Since 2001, he has been with Advanced Energy Industries, Inc., Fort Collins, CO.